Hindawi Publishing Corporation
Advances in High Energy Physics
Volume 2015, Article ID 914170, 14 pages
http://dx.doi.org/10.1155/2015/914170

*Research Article*

# Energy Dependence of Slope Parameter in Elastic Nucleon-Nucleon Scattering

**V. A. Okorokov**

*National Research Nuclear University MEPhI (Moscow Engineering Physics Institute), Kashirskoe Shosse 31, Moscow 115409, Russia*

Correspondence should be addressed to V. A. Okorokov; vaokorokov@mephi.ru

Received 25 June 2014; Revised 28 October 2014; Accepted 3 November 2014

Academic Editor: Bhartendu K. Singh



The diffraction slope parameter is investigated for elastic proton-proton and proton-antiproton scattering based on all the available experimental data at low and intermediate momentum transfer values. Energy dependence of the elastic diffraction slope is approximated by various analytic functions. The expanded "standard" logarithmic approximations with minimum number of free parameters allow description of the experimental slopes in all the available energy range reasonably. The estimations of asymptotic shrinkage parameter $\alpha'_{\mathscr{P}}$ are obtained for various $|t|$ domains based on all the available experimental data. Various approximations differ from each other both in the low energy and very high energy domains. Predictions for diffraction slope parameter are obtained for elastic proton-proton scattering from NICA up to future collider (FCC/VLHC) energies, for proton-antiproton elastic reaction in FAIR energy domain for various approximation functions.

## 1. Introduction

Elastic hadron-hadron scattering, the simplest type of hadronic collision process, remains one of the topical theoretical problems in the physics of fundamental interactions at present. Forward elastic scattering process is an excellent test for some fundamental principles (unitarity, analyticity, and asymptotic theorems) of modern approaches. In the case of $pp$ and $\overline{p}p$ elastic scattering, although many experiments have been made over an extended range of initial energies and momentum transfer, these reactions are still not well understood. One can suggests that, by the time the accelerator complexes like RHIC, LHC, and so forth are operating, the interest in the soft physics increases significantly. In the absence of a pure QCD description of the elastic $pp/\overline{p}p$ and these large-distance scattering states (soft diffraction), an empirical analysis based on model-independent fits to the physical quantities involved plays a crucial role [1]. Therefore, empirical fits of energy dependencies of global scattering parameters have been used as an important source of the model-independent information. This approach for $\sigma_{\text{tot}}$ and $\rho$ was used in [2, 3]. The third important quantity for nucleon elastic scattering is the slope parameter. The nuclear slope $B$ for elastic scattering is of interest in its own right. This quantity defined according to the following equation, $\alpha'_{\mathscr{P}}$,

$$B(s,t) = \frac{\partial}{\partial t}\left(\ln\frac{\partial\sigma(s,t)}{\partial t}\right), \tag{1}$$

is determined experimentally by fitting the differential cross-section $d\sigma/dt$ at some collision energy $\sqrt{s}$. On the other hand the study of $B$-parameter is important, in particular, for reconstruction procedure of full set of helicity amplitudes for elastic nucleon scattering [2, 3]. In the last 20–30 years, high energy $\overline{p}p$ colliders have extended the maximum $\overline{p}p$ collision energy from $\sqrt{s} \sim 20$ GeV to $\sqrt{s} \sim 2$ TeV, the LHC facility allows one to obtain $pp$ data up to $\sqrt{s} = 8$ TeV so far. As consequence, the available collection of $pp$ and $\overline{p}p$ slope data from literature has extended. The present status of slope for elastic $pp$ and $\overline{p}p$ scattering is discussed over the full energy domain. Predictions for further facilities are obtained based on the available experimental data.

## 2. Experimental Slope Energy Dependence

We have attempted to describe the energy behavior of the elastic nuclear slopes for $pp$ and $\overline{p}p$ reactions. The classical Pomeron theory gives in the first approximation the following expression for the differential cross-section of elastic scattering at asymptotically high energies:

$$\frac{d\sigma}{dt} \propto s^{2(\alpha_{\mathscr{P}}(t)-1)}, \tag{2}$$

where $\alpha_{\mathscr{P}}(t)$ is a Pomeron trajectory. If $\alpha_{\mathscr{P}}(t)$ is linear function of momentum transfer, that is, $\alpha_{\mathscr{P}}(t) = \alpha_{\mathscr{P}}(0) + \alpha'_{\mathscr{P}}t$, then for the slope parameter $B(s)$ at some $t$ using the definition (1) one can obtain

$$B(s) \propto 2\alpha'_{\mathscr{P}} \ln \varepsilon, \tag{3}$$

where $\varepsilon \equiv s/s_0$, $s_0 = 1\,\mathrm{GeV}^2$. In general case for Pomeron-inspired models the asymptotic shrinkage parameter $\alpha'_{\mathscr{P}}$ can be written as follows: $2\alpha'_{\mathscr{P}}(s) = \partial B(s,t)/\partial(\ln \varepsilon)$. Indeed the ensemble of experimental data for slope for elastic nucleon collisions can be approximated reasonably by many phenomenological approaches, at least for $\sqrt{s} > 20\,\mathrm{GeV}$. But models contradict with experimental data at lower energies and/or phenomenological approaches have a significant number of free parameters as usual. On the other hand it is apparent from previous investigations that the experimental data for slope parameter do not follow the straight lines at any initial energies when plotted as function of $\ln s$. The new "expanded" logarithmic parameterizations with small number of free parameters have been suggested in [2, 3, 5, 6] for description of the elastic slope at all available energies. Thus taking into account standard Regge parametrization and quadratic function of logarithm from [7] the following analytic equations are under study here:

$$B(s,t) = B_0 + 2a_1 \ln \varepsilon, \tag{4a}$$

$$B(s,t) = B_0 + 2a_1 \ln \varepsilon + a_2 \ln^{a_3} \varepsilon, \tag{4b}$$

$$B(s,t) = B_0 + 2a_1 \ln \varepsilon + a_2 \varepsilon^{a_3}, \tag{4c}$$

$$B(s,t) = B_0 + 2a_1 \ln \varepsilon + a_2 \ln^2 \varepsilon. \tag{4d}$$

In general parameters $B_0$, $a_i$, $i = 1 - 3$ depend on range of $|t|$ which is used for approximation. There are the relations $\alpha'_{\mathscr{P}} = a_1$ and $\alpha'_{\mathscr{P}} = a_1 + a_2 \ln \varepsilon$ for parameterizations (4a) and (4d) inspired by the Pomeron exchange models. As seen the function (4d) is the special case of (4b) at fixed value $a_3 = 2$. Additional terms in (4b)–(4d) take into account the nonlogarithmic part of the energy dependence of the elastic nuclear slopes. Approximation function (4c) is analogy of parametrization of momentum slope dependence from [8]. One can see that the parametrization (4c) is compatible to first order with the Regge pole model where the additional term represents the interference between the Pomeron and secondary trajectories [8].

Most of experimental investigations as well as theoretical models are focused on the diffraction region $|t| \lesssim 0.5\,\mathrm{GeV}^2$. In this paper we study all available experimental data for nuclear slope parameter up to $|t| \simeq 3.6\,\mathrm{GeV}^2$. Experimental values of slope parameter collected at initial energies $\sqrt{s} \leq 1.8\,\mathrm{TeV}$ are from [9]. Additional experimental results from Tevatron and the LHC are from [10] and [11–14], respectively. The full data sample consists of 490 experimental points. The number of experimental points equals 145/138 for $pp/\overline{p}p$ scattering at low $|t|$, respectively. In the intermediate $|t|$ domain experimental data set is 137/70 for $pp/\overline{p}p$ reaction, respectively. Thus the experimental sample is significantly larger than that in some early investigations [2, 3, 5–8, 15, 16]. The careful analysis of data sample allows us to suggest that the influence of double counting in the experimental data is negligible. It should be emphasized that the experimental data for intermediate $|t|$ range are separated on two samples which correspond to the various parametrization types for differential cross-section, namely, linear, $\ln(d\sigma/dt) \propto (-B|t|)$, and quadratic, $\ln(d\sigma/dt) \propto (-B|t| \pm Ct^2)$, function. Here $B, C > 0$ are suggested. As known the measurements of nuclear slope, especially at intermediate $|t|$, do not form a smooth set in energy, in contrast with the situation for global scattering parameters $\rho$ and $\sigma_{\mathrm{tot}}$, where there is a good agreement between various group data [7]. Detailed comparisons of slope data from different experiments are difficult because the various experiments cover different $|t|$ ranges, use various fitting procedures, and treat systematic errors in different ways, and, moreover, some experimental details are lost, especially, for very early data. We have tried to use as much as possible data for fit from available samples. But some of the $B$ values were not further used, either due to internal inconsistencies in the fitting procedure or as redundant in view of a better determination at a nearby initial energy. Thus the data samples for approximations are somewhat smaller because of exclusion of points which, in particular, differ significantly from the other experimental points at close energies. The choice of the range $|t|_{\min} \leq |t| \leq |t|_{\max}$ over which the fit of $d\sigma/dt$ is performed is important significantly for a consistent determination of slope parameters. It seems that both the mean value of $|t|$ ($|\bar{t}|$) and $|t|$-boundaries of corresponding measurements are important for separation of experimental results by different $|t|$ domains. Here the $|\bar{t}|$ is calculated taking into account the approximation of experimental $d\sigma/dt$ distribution instead of identifying of $|\bar{t}|$ with mean point of $|t|$-range as previously [5, 6]. Errors of experimental points include available clear indicated systematic errors added in quadrature to statistical ones. One needs to emphasize that the systematic errors caused by the uncertainties of normalization (total or/and differential cross-sections) are not taken into account if these uncertainties are not included in the systematic errors in the original papers.

Let us describe the fitting algorithm in more detail. We use the fitting procedure with standard likelihood function for this investigation of nuclear slope parameter. In accordance with [16] let us define the quantity

$$\Delta\chi_i^2(s_i;\boldsymbol{\alpha}) \equiv \left(\frac{B_m^i - B(s_i;\boldsymbol{\alpha})}{\sigma_i}\right)^2, \tag{5}$$

where $B^i_m$ is the measured value of nuclear slope at $s_i$, $B(s_i;\boldsymbol{\alpha})$ is the expected value from the one of the fitting functions under study, and $\sigma_i$ is the experimental error of the $i$th measurement. The parameters $\alpha_j$ are given by the $N$-dimensional vector $\boldsymbol{\alpha} = \{\alpha_1, \ldots, \alpha_N\}$. Our fitting algorithm is somewhat similar to the "sieve" algorithm from [16] with the following modification. We reject the points which *a priori* differ significantly from other experimental data at close energies. The step allows us to get a first estimation of $\chi^2$/n.d.f. with minimum number of rejected points. The fit quality is improved at the next steps consequently. As indicated above smoothness of experimental slope energy dependence differs significantly for data samples in various $|t|$-domains and for various parameterizations of $d\sigma/dt$ (see below). The absolute value of the $\Delta\chi^2_i(s_i;\boldsymbol{\alpha})$ can be large for one data sample but it can be acceptable for another sample at the same time. Therefore we suggest using the relative quantity

$$n_\chi = \frac{\Delta\chi^2_i(s_i;\boldsymbol{\alpha})}{\chi^2/\text{n.d.f.}} \tag{6}$$

in order to reject the outliers (points far off from the fit curve for the certain data sample) instead of constant cut value $\Delta\chi^2_i(s_i;\boldsymbol{\alpha})_{\max}$ from the "sieve" algorithm [16]. One needs to emphasize that the fit function with best $\chi^2$/n.d.f. for description of all range of available energies among (4a)–(4d) is used for calculation of the expected value in (5) at each algorithm step and then for estimation of (6) quantity. The points with $n_\chi \geq n^{\max}_\chi$ are excluded from future study in our algorithm, where the $n^{\max}_\chi$ is some empirical cut value. The conventional fit is made to the new "sifted" data sample. We consider the estimates of fit parameters as the final results if there are no excluded points for present data sample. We use the one value $n^{\max}_\chi = 2$ for all data samples considered in this paper below. The fraction of excluded points is about 2% for $pp$ as well as for $\overline{p}p$ elastic scattering for low $|t|$ domain. The maximum relative amount of rejected points is about 3%/12% for linear $\ln d\sigma/dt$ parametrization and 6%/15% for quadratic one at intermediate $|t|$ values for $pp/\overline{p}p$ scattering, respectively.

*2.1. Low $|t|$ Domain.* The energy dependence for experimental slopes and corresponding fits by (4a)–(4d) is shown at Figures 1 and 2 for $pp$ and $\overline{p}p$, respectively. The values of fit parameters are shown in Table 1. One can see that the fitting functions (4a) and (4d) describe the $pp$ (Figure 1) and $\overline{p}p$ (Figure 2) experimental data statistically acceptable only for $\sqrt{s} \geq 5$ GeV. Additional study demonstrates that the extension of approximation domain down to the lower energies for parameterizations (4a) and (4d) results in significant increasing of $\chi^2$/n.d.f. for both $pp$ and $\overline{p}p$ data samples. Thus these fit functions allow one to get reasonable fit qualities only at $\sqrt{s} \geq 5$ GeV for $\overline{p}p$ scattering as well as for elastic $pp$ reaction.

The RHIC point for $pp$ collisions does not contradict the common trend within large error bars and cannot discriminate the approximations under study. In general the LHC results

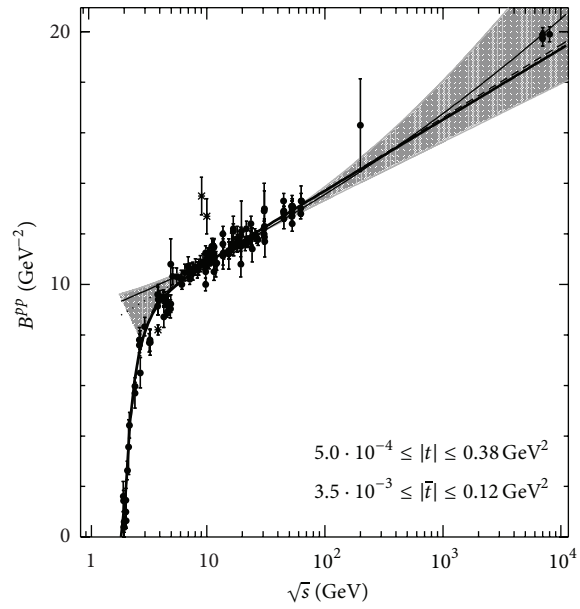


Figure 1: Energy dependence of the elastic slope parameter for proton-proton scattering for low $|t|$ domain. Experimental points from fitted samples are indicated as •; unfitted points are indicated as ∗. The dot curve is the fit of experimental slope by the function (4a), thick solid—by (4b), dashed—by (4c), thin solid—by (4d). The shaded band corresponds to the spread of fitting functions for previous analysis [9].

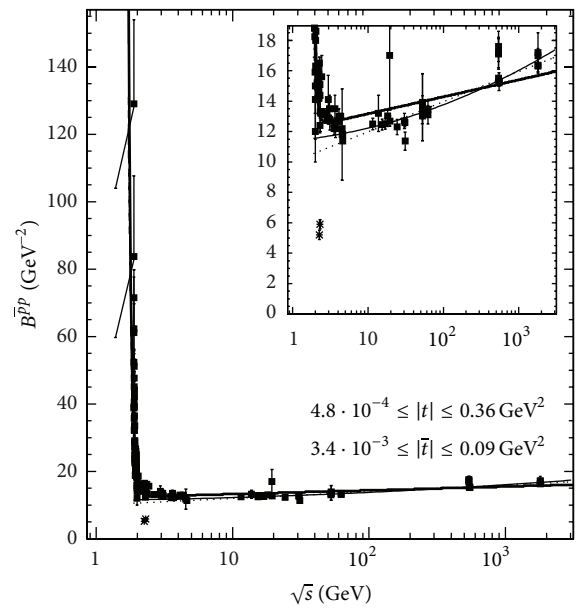


Figure 2: Energy dependence of the elastic slope parameter for antiproton-proton scattering for low $|t|$ domain. Experimental points from fitted samples are indicated as ■, unfitted points are indicated as ∗. The correspondence of curves to the fit functions is the same as well as in Figure 1. The inner picture shows the experimental data and fits for the same scale of slope as well as in Figure 1.

Table 1: Values of parameters for fitting of slope energy dependence in low $|t|$ domain.

| Function | Parameter | | | | |
|---|---|---|---|---|---|
| | $B_0$, GeV$^{-2}$ | $a_1$, GeV$^{-2}$ | $a_2$, GeV$^{-2}$ | $a_3$ | $\chi^2$/n.d.f. |
| | | | Proton-proton scattering | | |
| (4a) | 8.00 ± 0.06 | 0.309 ± 0.010 | — | — | 234/98 |
| (4b) | 8.09 ± 0.06 | 0.305 ± 0.005 | −31.8 ± 1.6 | −4.06 ± 0.13 | 420/138 |
| (4c) | 7.95 ± 0.06 | 0.313 ± 0.005 | −240 ± 32 | −2.23 ± 0.09 | 402/138 |
| (4d) | 8.81 ± 0.12 | 0.198 ± 0.015 | 0.013 ± 0.002 | — | 174/97 |
| | | | Proton-antiproton scattering | | |
| (4a) | 10.0 ± 0.2 | 0.215 ± 0.012 | — | — | 32/27 |
| (4b) | 12.02 ± 0.06 | 0.121 ± 0.006 | 495 ± 98 | −13.0 ± 0.5 | 1220/132 |
| (4c) | 12.06 ± 0.05 | 0.119 ± 0.005 | $(3.1 \pm 0.4) \cdot 10^6$ | −9.36 ± 0.10 | 1303/132 |
| (4d) | 11.4 ± 1.0 | 0.05 ± 0.11 | 0.017 ± 0.011 | — | 29/26 |

[12–14] added in fitting sample result in better agreement of fits (4a)–(4d) in comparison with previous study [9]. All fits are very close to each other in energy domain $10\,\text{GeV} \lesssim \sqrt{s} \lesssim 1\,\text{TeV}$; the quadratic function (4d) shows somewhat faster increasing of slope and noticeable difference from other fit functions in multi-TeV region only. It seems the ultra-high energy domain is suitable for separation of various parameterizations. Fitting functions (4b) and (4c) allow us to describe experimental data at all energies with reasonable fit quality for $pp$ (Table 1). The functions (4a)–(4c) agree very well for $\sqrt{s} \geq 5\,\text{GeV}$; furthermore there is no visible difference between modifications (4b) and (4c) in all experimentally available energy domains. The function (4c) demonstrates some better quality for fit of full data sample (Table 1) than function (4b) in contrast with previous analysis [9]. The accounting for LHC data leads to some decreasing of values of $B_0$ and increasing of $a_1$ parameters for all fitting functions (4a)–(4d) under study in comparison with values of corresponding parameters in previous investigation [9]. This behavior of $a_1$ with collision energy agrees well with predicted growth of $\alpha'_{\mathcal{P}}$ with increasing of $\sqrt{s}$ [17, 18]. As seen from Table 1 the third term in both (4b) and (4c) gives the main contribution at $\sqrt{s} < 5\,\text{GeV}$ in the case of elastic proton-proton scattering, that is, describing the sharp changing of slope in the low energy domain. Therefore $B^{pp} \propto \ln \varepsilon$ at high $\sqrt{s}$ in accordance with (4b) and (4c). The increasing of $a_1$ exhibits that $B^{pp}$ grows somewhat faster in multi-TeV region than one can expect from the trend based on data sample at $\sqrt{s} \leq 200\,\text{GeV}$. This suggestion is confirmed by improvement of fit quality for one fitting function (4d) for present data sample in comparison with fit qualities for experimental points at $\sqrt{s} \leq 200\,\text{GeV}$ [9]. Values of $a_2$ obtained in the present study and for fit at $\sqrt{s} \leq 200\,\text{GeV}$ are close within errors for functions (4b) and (4d) but accounting for the LHC data results in some increasing of the absolute value of $a_3$ in fit by (4b). The absolute values of $a_2$ and $a_3$ are the same within error bars for function (4c) for Table 1 and for fit in energy domain $\sqrt{s} \leq 200\,\text{GeV}$ [9].

As seen from Table 1 values of $a_1$ parameter obtained for slope in elastic $pp$ scattering are significantly larger than thaose for elastic $\overline{p}p$ reactions for any approximations (4a)–(4d) under study. The parameter $a_1$ for Regge-inspired function (4a) is close to estimation for Pomeron parameter $\alpha'_{\mathcal{P}} \approx 0.25\,\text{GeV}^{-2}$ for $\overline{p}p$. The $a_1^{pp}$ values from Table 1 coincided within error bars for fitting function (4a)–(4c). These values are larger than earlier experimental estimations of "true" Pomeron shrinkage parameter [19]. Also the value of $a_1^{pp}$ parameter for fitting function (4c) exceeds significantly the value of corresponding parameter for such fit of slope momentum dependence but in much narrower energy range $\sqrt{s} \lesssim 60\,\text{GeV}$ [8]. Thus the comparison with earlier estimations confirms the conclusion made above that the including of high energy data points into fitted sample leads to the increasing of value of the $a_1^{pp}$ parameter and growth of slope parameter seems to be faster in TeV-region than that at lower energies. Accordingly the $a_1^{pp}$ value for function (4d) is significantly closer to the $\alpha'_{\mathcal{P}} \approx 0.25\,\text{GeV}^{-2}$ than that for previous analysis in energy range $\sqrt{s} \leq 200\,\text{GeV}$ [9]. On the other hand the values of the $a_1^{pp}$ parameter obtained for fitting function (4a) are somewhat larger than the prediction for $\alpha'_{\mathcal{P}}$ from Pomeron-inspired model for TeV-energy domain [18]. Furthermore the proton-proton results from fit by function (4d) allow the estimation $2\alpha'_{\mathcal{P}}(s)|_{\sqrt{s}=8\,\text{TeV}} = 0.86 \pm 0.08$ which is almost twice larger than the corresponding prediction from [18].

The qualities of (4b) and (4c) approximation functions for $\overline{p}p$ elastic scattering data are much poorer because of very sharp behavior of experimental data near the low energy boundary. But one can see that the functions (4b) and (4c) agree with experimental points at qualitative level and are (very) close to each other for all energy range. In contrast with elastic $pp$ scattering the fit quality is somewhat better for function (4b) than for parametrization (4c) for $\overline{p}p$ data. Additional study of antiproton-proton data shows that the increasing of low boundary of range of fitted energies ($s_{\min}$) leads to the better fit quality for functions (4b) and (4c) but at the same time, obviously, to the loss of some low-energy $\overline{p}p$ data. The fit quality changes dramatically at small increasing of $s_{\min}$ from low boundary value $4m_p^2$ to $3.72\,\text{GeV}^2$. It was obtained $\chi^2$/n.d.f. $\simeq 5.4/5.5$ for function (4b)/(4c), respectively, for fit range $s_{\min} \geq 3.72\,\text{GeV}^2$. On the other hand the corresponding data sample is about 75% from the maximum one in this case. Thus it seems that

Table 2: Predictions for slope in nucleon-nucleon elastic scattering at intermediate energies for low $|t|$ domain.

| Fitting function | Facility energies $\sqrt{s}$, GeV | | | | | |
|---|---|---|---|---|---|---|
| | FAIR | | | | NICA | |
| | 3 | 5 | 6.5 | 14.7 | 20 | 25 |
| (4a) | — | $11.4 \pm 0.2$ | $11.6 \pm 0.2$ | $12.3 \pm 0.2$ | $11.70 \pm 0.13$ | $11.98 \pm 0.14$ |
| (4b) | $12.57 \pm 0.07$ | $12.80 \pm 0.07$ | $12.93 \pm 0.07$ | $13.32 \pm 0.09$ | $11.72 \pm 0.08$ | $12.00 \pm 0.09$ |
| (4c) | $12.59 \pm 0.05$ | $12.83 \pm 0.06$ | $12.95 \pm 0.06$ | $13.34 \pm 0.07$ | $11.70 \pm 0.08$ | $11.98 \pm 0.09$ |
| (4d) | — | $11.9 \pm 1.2$ | $12.0 \pm 1.3$ | $12.4 \pm 1.6$ | $11.6 \pm 0.2$ | $11.9 \pm 0.2$ |

Table 3: Predictions for slope in $pp$ elastic scattering at high energies for low $|t|$ domain.

| Fitting function | Facility energies $\sqrt{s}$, TeV | | | | | | |
|---|---|---|---|---|---|---|---|
| | RHIC | LHC | | | FCC/VLHC | | |
| | 0.5 | 14 | 28 | 42* | 100 | 200 | 500 |
| (4a) | $15.7 \pm 0.3$ | $19.8 \pm 0.4$ | $20.7 \pm 0.4$ | $21.2 \pm 0.4$ | $22.2 \pm 0.5$ | $23.1 \pm 0.5$ | $24.2 \pm 0.5$ |
| (4b) | $15.67 \pm 0.14$ | $19.7 \pm 0.2$ | $20.6 \pm 0.2$ | $21.1 \pm 0.2$ | $22.1 \pm 0.2$ | $23.0 \pm 0.3$ | $24.1 \pm 0.3$ |
| (4c) | $15.73 \pm 0.14$ | $19.9 \pm 0.2$ | $20.8 \pm 0.2$ | $21.3 \pm 0.2$ | $22.4 \pm 0.2$ | $23.2 \pm 0.3$ | $24.4 \pm 0.3$ |
| (4d) | $15.7 \pm 0.5$ | $21.1 \pm 0.9$ | $22.4 \pm 1.0$ | $23.1 \pm 1.1$ | $24.8 \pm 1.3$ | $26.2 \pm 1.4$ | $28.2 \pm 1.6$ |

*The ultimate energy upgrade of LHC project [4].

the $s_{\min} = 3.72\,\text{GeV}^2$ is one of the optimum values from point of view of both the fit quality and the closing to the threshold $s_{\min} = 4m_p^2$. The average value of (6) for excluded points is equal to 4.7 for $pp$ and 65.8 for $\overline{p}p$ data sample for parametrization (4c).

Predictions for nuclear slope parameter values for some facilities have been obtained based on the fit results shown above. The $B$ estimations at low $|t|$ for different intermediate energies of the projects FAIR and NICA are shown in Table 2 and those for high energy domain are presented in Table 3. As expected the functions (4b) and (4c) predict for FAIR that the $B$ values coincide with each other within errors. The approximation functions (4a) and (4d) can be predicted for $\sqrt{s} \geq 5\,\text{GeV}$ only. The Regge-inspired function (4a) predicts slope parameter values significantly smaller than those for modified fitting functions (4b) and (4c) at FAIR energies. Predictions with help of quadratic function (4d) of $\ln \varepsilon$ are equal with estimations based on any other fitting function under study within large error bars at $\sqrt{s} \leq 14.7\,\text{GeV}$. In the case of elastic $pp$ scattering the functions (4a)–(4c) predict just the equal values of $B$ within error bars at any collision energy $\sqrt{s}$ discussed here. The difference between estimations from (4a)–(4c) and from (4d) onsets at the final energy of the LHC project $\sqrt{s} = 14\,\text{TeV}$ only. Our prediction with (4d) function for RHIC energy is equal to early prediction for close energy based only on slope data in the region $5 < \sqrt{s} < 62\,\text{GeV}$ [7] within errors. But (4d) underestimates the $B$ values in ultra-high energy domain $\sqrt{s} > 40\,\text{TeV}$ in comparison with results based on the approach without Odderons [7]. It should be emphasized that in contrast with previous analysis [9] the present fits by functions (4a)–(4d) of data sample included results from the LHC predict similar increasing of $B$ with energy to most of phenomenological models [20]. The $B$ value predicted for the LHC at $\sqrt{s} = 14\,\text{TeV}$ by (4a) only is close to errors to the predictions from [21, 22], in particular, with estimation from model with hadronic amplitude corresponding to the exchange of two Pomerons. Prediction of phenomenological model with hadronic amplitude corresponding to the exchange of three Pomerons [22] at $\sqrt{s} = 14\,\text{TeV}$ coincides with estimation of $B$ within error bars from fit function (4d) with the fastest growth of $B$ with $\sqrt{s}$ in multi-TeV region. But most of estimations of $B$ at $\sqrt{s} = 14\,\text{TeV}$ from Table 3 agree well within errors with model prediction from [23]. However the model estimates at $\sqrt{s} = 14\,\text{TeV}$ described above were obtained for $B(t = 0)$ and the $t$-dependence of slope shows the slight decreasing of $B$ for the model with three-Pomeron exchange [22] and faster decreasing of $B$ for the model from [23] at growth of momentum transfer up to $|t| \approx 0.1\,\text{GeV}^2$. Therefore one can expect that the model with hadronic amplitude corresponding to the exchange of three Pomerons [22] will be in better agreement with values of $B$ from Table 3 predicted for finite (nonzero) low $|t|$ values. But the model from [24] overestimates the $B$ value at $\sqrt{s} = 14\,\text{TeV}$ in comparison with the corresponding predictions from fitting functions (4a)–(4d) despite the sharp decreasing of $B$ at growth of momentum transfer up to $|t| \approx 0.1\,\text{GeV}^2$ in this model. As suggested sometimes the saturation regime, Black Disk Limit (BDL), may be reached at the LHC. One of the models in which such effects appear, namely, Dubna Dynamical Model (DDM), predicts the slope $B(t = 0) \approx 23.5\,\text{GeV}^{-2}$ at $\sqrt{s} = 14\,\text{TeV}$ [25] which is noticeably larger than the predictions from Table 3 at the same $\sqrt{s}$. Therefore the saturation regime will not be reached, at least, at the LHC energy $\sqrt{s} = 14\,\text{TeV}$ as suggested, for example, in the model from [26], or simple saturation can not be enough in order to describe the LHC data at quantitative level.

*2.2. Intermediate $|t|$ Domain.* As indicated above the situation is more complicated for intermediate $|t|$ domain. Differential cross-section is approximated by linear, $\ln(d\sigma/dt) \propto (-B|t|)$,

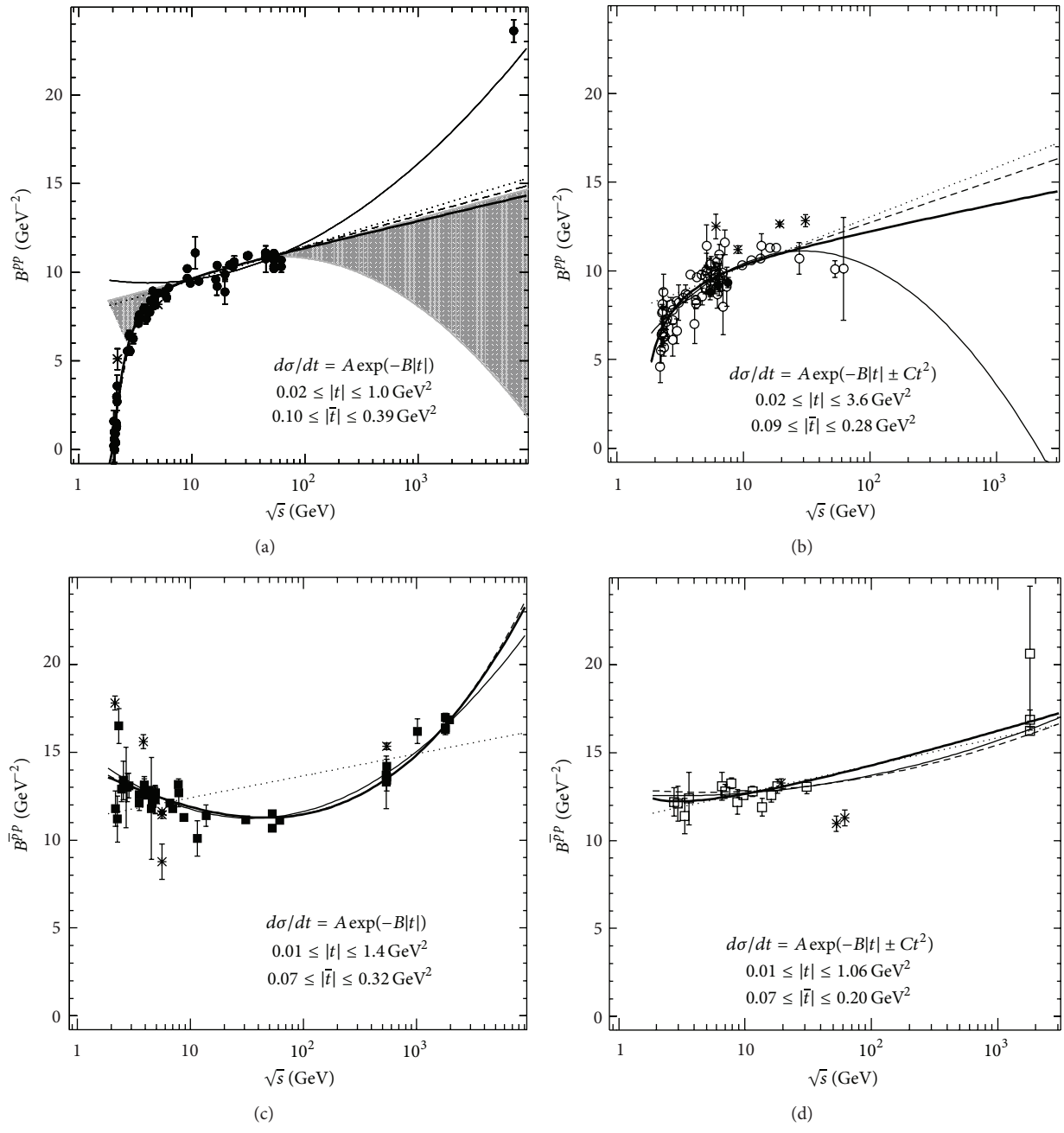


FIGURE 3: Energy dependence of $B$ in proton-proton (a, b) and proton-antiproton (c, d) elastic scattering for linear (a, c) and quadratic (b, d) exponential parametrization of differential cross-section. Experimental points from fitted samples are indicated as close/open circles (squares) for $pp$ ($\overline{p}p$) for (a, c)/(b, d); unfitted points are indicated as $*$. The dot curve is the fit of experimental slope by the function (4a), thick solid—by (4b), dashed—by (4c), and thin solid—by (4d). The shaded band (a) corresponds to the spread of fitting functions for previous analysis [9].

and/or quadratic, $\ln(d\sigma/dt) \propto (-B|t| \pm Ct^2)$, function in various experiments; $|t|$ ranges used for $d\sigma/dt$ approximations differ significantly, and so forth. For quadratic exponential parametrization the $B$ and $C$ parameters are highly correlated by fits.

Figure 3 shows the experimental data and corresponding fits for energy dependence of slope parameter at intermediate $|t|$ for $pp$ and $\overline{p}p$ elastic scattering. Figures 3(a) and 3(c) correspond to the linear exponential approximation of differential cross-section for $pp$ and $\overline{p}p$, respectively. Experimental data obtained at quadratic exponential fit of $d\sigma/dt$ and fitting functions (4a)–(4d) are presented in Figure 3(b) for $pp$ and in Figure 3(d) for $\overline{p}p$ collisions. The fitting parameter values are indicated in Table 4 for various interaction types and for different $d\sigma/dt$ parameterizations. Usually the fit qualities are poorer for intermediate $|t|$ values than those for low $|t|$ range

Table 4: Values of parameters for fitting of energy dependence of slope at intermediate $|t|$.

| Function | Parameter | | | | |
|---|---|---|---|---|---|
| | $B_0$, GeV$^{-2}$ | $a_1$, GeV$^{-2}$ | $a_2$, GeV$^{-2}$ | $a_3$ | $\chi^2$/n.d.f. |
| Proton-proton scattering, experimental data for $d\sigma/dt = A\exp(-B\|t\|)$ | | | | | |
| (4a) | 7.59 ± 0.11 | 0.211 ± 0.008 | — | — | 322/35 |
| (4b) | 8.39 ± 0.17 | 0.163 ± 0.011 | −25.2 ± 1.4 | −3.01 ± 0.13 | 493/61 |
| (4c) | 7.94 ± 0.11 | 0.19 ± 0.09 | −90 ± 8 | −1.69 ± 0.06 | 458/61 |
| (4d) | 9.9 ± 0.2 | −0.16 ± 0.03 | 0.056 ± 0.005 | — | 187/34 |
| Proton-proton scattering, experimental data for $d\sigma/dt = A\exp(-B\|t\| \pm Ct^2)$ | | | | | |
| (4a) | 7.4 ± 0.2 | 0.31 ± 0.03 | — | — | 115/33 |
| (4b) | 9.6 ± 2.4 | 0.16 ± 0.13 | −7.2 ± 5.4 | −1.5 ± 1.0 | 227/62 |
| (4c) | 7.9 ± 0.5 | 0.26 ± 0.05 | −23 ± 16 | −1.5 ± 0.5 | 228/62 |
| (4d) | 4.1 ± 0.9 | 1.0 ± 0.2 | −0.15 ± 0.04 | — | 102/32 |
| Proton-antiproton scattering, experimental data for $d\sigma/dt = A\exp(-B\|t\|)$ | | | | | |
| (4a) | 11.16 ± 0.06 | 0.136 ± 0.004 | — | — | 1168/42 |
| (4b) | 14.34 ± 0.11 | −0.304 ± 0.014 | 0.0042 ± 0.0004 | 2.92 ± 0.04 | 186/40 |
| (4c) | 7.7 ± 0.2 | −0.735 ± 0.019 | 6.9 ± 0.2 | 0.1000 ± 0.0013 | 188/40 |
| (4d) | 15.48 ± 0.15 | −0.60 ± 0.02 | 0.084 ± 0.003 | — | 197/41 |
| Proton-antiproton scattering, experimental data for $d\sigma/dt = A\exp(-B\|t\| \pm Ct^2)$ | | | | | |
| (4a) | 11.1 ± 0.2 | 0.171 ± 0.011 | — | — | 17.3/15 |
| (4b) | $(-1 \pm 3)\cdot 10^3$ | 0.26 ± 0.06 | $(1 \pm 3)\cdot 10^3$ | −0.001 ± 0.004 | 14.5/13 |
| (4c) | $(-2.2 \pm 1.8)\cdot 10^2$ | 1.7 ± 0.8 | $(2.3 \pm 1.8)\cdot 10^2$ | −0.015 ± 0.006 | 13.2/13 |
| (4d) | 12.7 ± 0.8 | −0.05 ± 0.11 | 0.023 ± 0.011 | — | 13.2/14 |

in $pp$ elastic collisions for linear exponential parametrization of $d\sigma/dt$. The fitting functions (4a) and (4d) agree with experimental points qualitatively both for linear (Figure 3(a)) and quadratic (Figure 3(b)) exponential parameterizations of $d\sigma/dt$ for $\sqrt{s} \geq 5$ GeV only. The "expanded" functions (4b) and (4c) approximate experimental data at all energies reasonably with close fit qualities, especially for quadratic exponential parametrization of $d\sigma/dt$ (Table 4). But (4b) function shows a very slow growth of slope parameter with energy increasing at $\sqrt{s} \geq 100$ GeV (Figure 3(a)). It should be stressed that the experimental point at the LHC energy leads to the dramatic change of behavior of the fitting function (4d) in comparison with previous analysis [9]. At present the fitting function (4d) predicts increasing of the nuclear slope in high energy domain as well as all other fitting functions under study. Such behavior is opposite to the result of fit by function (4d) of experimental data sample at $\sqrt{s} \leq 200$ GeV [9]. In the case of linear exponential approximation of $d\sigma/dt$ mean value of characteristic (6) is about 2.9 for excluded $pp$ data points with (4c) function and $\overline{n_\chi} = 18.3$ for points excluded from $\overline{p}p$ fitted data sample for (4b) fitting function.

One can see that the $\overline{p}p$ experimental data admit the approximation by (4d) for all energy range but not only for $\sqrt{s} \geq 5$ GeV. Indeed the fit quality for the first case is much better than that for second one. Additional analysis demonstrated just the same behavior of fit quality for function (4a) too. Thus $\overline{p}p$ experimental points from linear exponential parametrization of differential cross-section are fitted by (4a) and (4d) at all energies not only for $\sqrt{s} \geq 5$ GeV. The parameter values are shown in Table 4 for approximation by (4a) and (4d) of all available experimental data. The fit curves show (very) close behaviors for both the present and previous analyses in the case of Figure 3(c). The $\overline{p}p$ data disagree with Regge-inspired fitting function very significantly (Figure 3(c)). Functions (4b) and (4c) show a very close behavior at all energies for $\overline{p}p$ data from linear parametrization of $\ln d\sigma/dt$. These fitting functions have a better fit quality than (4d) but fits by functions (4b) and (4c) are still statistically unacceptable. As previously experimental data at Figure 3(d) allow the approximation by (4a) and (4d) for all energy range but not only for $\sqrt{s} \geq 5$ GeV. The fit qualities are better in the first case of energy range and fitting parameters are indicated in Table 4, namely, for this energy range. In contrast with the case of linear parametrization of $\ln d\sigma/dt$ for $\overline{p}p$ here the functions (4c) and (4d) show a close fit quality which is somewhat better than this parameter for (4b) fitting function. One can see the fit qualities for (4a)–(4d) are better significantly for data from quadratic exponential parametrization of differential cross-sections than for data from linear exponential approximation of $d\sigma/dt$. Thus fitting functions (4c) and (4d) agree with data points at quantitative level for quadratic parametrization of proton-antiproton $\ln d\sigma/dt$ (Figure 3(d)) and these fits are statistically acceptable. Excluded points are characterized by $\overline{n_\chi} \simeq 17.9$ for $pp$ data with (4b) fitting function and by $\overline{n_\chi} \simeq 12.1$ for $\overline{p}p$ data sample at (4d) function.

From the quadratic exponential parametrization of differential cross-section one may calculate the local slope at a certain $|t|$-value via the following relation:

$$b(s,t) = B \pm C\ln|t|, \quad B, C > 0. \tag{7}$$

This characteristic can be useful for elastic scattering for study of $d\sigma/dt$ in wider $|t|$ range. It is suggested $b \geq 0$

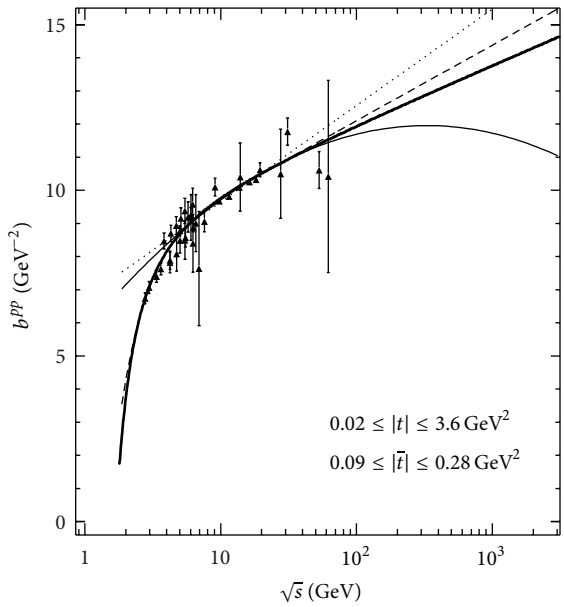


FIGURE 4: Energy dependence of the slope parameter $b$ at $|t| = 0.2\,\text{GeV}^2$ for proton-proton scattering. The correspondence of curves to the fit functions is the same as that in Figure 1.

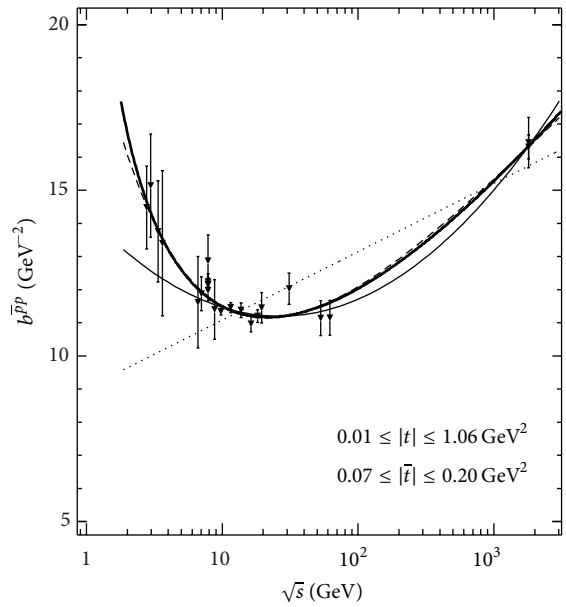


FIGURE 5: Energy dependence of the slope parameter $b$ at $|t| = 0.2\,\text{GeV}^2$ for antiproton-proton scattering. The correspondence of curves to the fit functions is the same as that in Figure 1.

according to definition (7). The $b$-parameter is named slope too; it is evaluated at $|t| = 0.2\,\text{GeV}^2$ usually. One of the advantages of this characteristic is the expectation of more smooth energy (momentum) dependence than that for $B$-parameter discussed above. Indeed we have included the 100% of available experimental points in fitted sample for $pp$ elastic scattering. But the number of points is somewhat smaller than that for $B$-parameter because of absent $C$-parameter values for some low energy measurements from [15]. We excluded one point at $\sqrt{s} = 1.8\,\text{TeV}$ [27] from fitted sample for $\overline{p}p$ elastic reaction because there are unacceptably large errors (relative error is $\delta b \simeq 2.72$) for this point.

Experimental values of $b$ depend on collision energy and corresponding fits are shown in Figure 4 for $pp$ elastic scattering and in Figure 5 for $\overline{p}p$ collisions. In the last case fit qualities for (4a) and (4d) functions are better for fitting at $\sqrt{s} \ge 5\,\text{GeV}$ only than for fitting of all available energy domain. The fit parameter values are shown in Table 5. Fit qualities are significantly better than those for corresponding fits of $B$-parameter with the exception of (4a) for $\overline{p}p$ data. Functions (4a) and (4d) approximate $b(\sqrt{s})$ for $pp$ data statistically acceptable for $\sqrt{s} \ge 5\,\text{GeV}$ only. Functions (4b) and (4c) show acceptable close fit qualities and difference at high energies only. The shrinkage parameter $a_1^{pp}$ for approximation function (4c) with best fit quality is in a good agreement with the early results [8]. Function (4b) shows a best fit quality for $\overline{p}p$ data. Thus the "expanded" parameterizations (4b) and (4c) suppose statistically acceptable representation of all available experimental data for $b$-parameter both in $pp$ and $\overline{p}p$ elastic reactions.

We have obtained predictions for nuclear slope parameters $B$ and $b$ for some facilities and intermediate $|t|$ based on the fit results shown above. The predicted $B$ values at intermediate $|t|$ are calculated on the base of fitting parameters obtained for linear exponential parametrization of $d\sigma/dt$. Slope values are shown in Table 6 for different energies of FAIR and NICA and in Table 7 for RHIC, LHC, and FCC/VLHC. According to the fit range function (4a) can predict the $B$ value for $\overline{p}p$ scattering at all energies under study not in $\sqrt{s} \ge 5\,\text{GeV}$ domain only. As expected the functions (4b)–(4d) predicted very close values for slope parameter $B$ for FAIR. These fitting functions, especially (4b) and (4c), predict the close values for nuclear slope $B$ in NICA energy domain too. Functions (4a)–(4c) predict smaller values for $B$ in high energy $pp$ collisions than (4d) approximation especially for FCC/VLHC energy domain. Perhaps, the future more precise RHIC results will be useful for discrimination of fitting functions under study for intermediate $|t|$ values. In contrast with previous analysis [9], here the function (4d) with obtained parameters predicts fast growth of $B$ values at energies of future experiments. This behavior of estimations calculated for functions (4a)–(4d) contradicts with earlier predictions from some phenomenological models. It should be emphasized that various phenomenological models predict a very sharp decreasing of nuclear slope in the range $|t| \sim 0.3$–$0.5\,\text{GeV}^2$ at LHC energy $\sqrt{s} = 14\,\text{TeV}$ [20]. Just the positive $B$ value predicted for LHC at $\sqrt{s} = 14\,\text{TeV}$ by (4d) is most close to the some model expectations [22, 23]. Taking into account predictions in Table 2 based on the fitting functions (4a)–(4d) for low $|t|$ one can suggest that the model with hadronic amplitude corresponding to the exchange of three Pomerons [20, 22] describes the nuclear slope somewhat closer to the experimentally inspired values at LHC energy both at low and intermediate $|t|$ than other models. The situation with predictions for $b$ at intermediate energies is similar to that for $B$: functions (4b)–(4d) predict

Table 5: Values of parameters for fitting of the $b$ energy dependence.

| Function | Parameter | | | | |
|---|---|---|---|---|---|
| | $B_0$, GeV$^{-2}$ | $a_1$, GeV$^{-2}$ | $a_2$, GeV$^{-2}$ | $a_3$ | $\chi^2$/n.d.f. |
| | | | Proton-proton scattering | | |
| (4a) | 6.7 ± 0.2 | 0.32 ± 0.02 | — | — | 25.6/25 |
| (4b) | 9 ± 2 | 0.19 ± 0.12 | −10 ± 2 | −1.9 ± 0.5 | 41.5/33 |
| (4c) | 7.6 ± 0.8 | 0.25 ± 0.07 | −20 ± 4 | −1.16 ± 0.14 | 41.4/33 |
| (4d) | 5.8 ± 0.9 | 0.53 ± 0.19 | −0.046 ± 0.015 | — | 24.3/24 |
| | | | Proton-antiproton scattering | | |
| (4a) | 9.2 ± 0.2 | 0.22 ± 0.02 | — | — | 40.5/13 |
| (4b) | 50.8 ± 0.9 | 0.92 ± 0.06 | −34.1 ± 0.8 | 0.222 ± 0.016 | 8.7/15 |
| (4c) | 2.4 ± 1.6 | 0.46 ± 0.11 | 18.5 ± 2.3 | −0.29 ± 0.11 | 9.0/15 |
| (4d) | 14 ± 1 | −0.47 ± 0.12 | 0.07 ± 0.01 | — | 8.1/12 |

Table 6: Predictions for slopes in nucleon-nucleon elastic scattering at intermediate energies for intermediate $|t|$ domain.

| Fitting function | Facility energies $\sqrt{s}$, GeV | | | | | |
|---|---|---|---|---|---|---|
| | FAIR | | | | NICA | |
| | 3 | 5 | 6.5 | 14.7 | 20 | 25 |
| | | | $B$-parameter | | | |
| (4a) | 11.76 ± 0.06 | 12.04 ± 0.07 | 12.18 ± 0.07 | 12.62 ± 0.07 | 10.12 ± 0.15 | 10.31 ± 0.15 |
| (4b) | 12.88 ± 0.13 | 12.51 ± 0.14 | 12.26 ± 0.15 | 11.6 ± 0.2 | 10.2 ± 0.2 | 10.4 ± 0.2 |
| (4c) | 13.1 ± 0.3 | 12.5 ± 0.4 | 12.2 ± 0.4 | 11.6 ± 0.5 | 10.2 ± 1.1 | 10.4 ± 1.2 |
| (4d) | 13.27 ± 0.18 | 12.5 ± 0.2 | 12.2 ± 0.2 | 11.5 ± 0.3 | 10.0 ± 0.5 | 10.1 ± 0.5 |
| | | | $b$-parameter | | | |
| (4a) | 10.0 ± 0.2 | 10.5 ± 0.2 | 10.7 ± 0.3 | 11.4 ± 0.3 | 10.5 ± 0.3 | 10.8 ± 0.4 |
| (4b) | 14.3 ± 1.4 | 12.6 ± 1.7 | 12.0 ± 1.8 | 11 ± 2 | 10 ± 2 | 11 ± 3 |
| (4c) | 14 ± 3 | 13 ± 3 | 12 ± 3 | 11 ± 3 | 10.5 ± 1.1 | 10.7 ± 1.2 |
| (4d) | 12.6 ± 1.1 | 12.0 ± 1.2 | 11.8 ± 1.3 | 11.3 ± 1.7 | 10 ± 2 | 11 ± 3 |

close values for $b$ within large errors for both the FAIR and the NICA. Furthermore all fitting functions predict the close values of $b$ at $\sqrt{s} > 5$ GeV. The value of $b$-parameter obtained from function (4a) differs significantly from estimations with other fitting functions for $\overline{p}p$ elastic scattering at low energies. Therefore the $b$-parameter seems more perspective for distinguishing of Regge-inspired function (4a) from "expanded" parameterizations (4b)-(4c) at $\sqrt{s} \sim 3$ GeV than $B$. One can see the functions (4b) and (4c) predict very close values of $b$ in high energy domain. Function (4d) shows a decreasing of $b$ at high energies in the contrast with $B$-parameter. In general estimations for $b$-parameter in Table 7 agree within errors for all fitting functions under study up to the $\sqrt{s} = 14$ TeV. But the large errors for function (4d) do not allow the unambiguous physics conclusion especially at the LHC energies and above.

*2.3. $\Delta B$ and NN Data Analysis.* Phenomenological models predict the zero difference of slopes ($\Delta B$) for proton-antiproton and proton-proton elastic scattering at asymptotic energies. Here the difference $\Delta B$ is calculated for all functions (4a)–(4d) under study with parameters corresponding to $\overline{p}p$ and $pp$ fits: $\Delta B_i(s) = B_i^{\overline{p}p}(s) - B_i^{pp}(s)$, $i$ = (4a)–(4d). (Obviously, one can suggest various combinations of fitting functions for $\Delta B$ calculations, for example, the difference between fitting functions with best fit qualities, etc.) It should be stressed that the equal energy domain is used in $\overline{p}p$ and $pp$ fits for $\Delta B$ calculations; that is, the parameter values obtained by (4d) fitting function for $\overline{p}p$ data from linear exponential fit of $d\sigma/dt$ for $\sqrt{s} \geq 5$ GeV are used for corresponding $\Delta B$ definition. The energy dependence of $\Delta B$ is shown in Figures 6(a) and 6(b) for low and intermediate $|t|$, respectively. One can see that the difference of slopes decreases with increasing of energy for low $|t|$ domain (Figure 6(a)) as well as in the previous analysis [9]. The fitting functions (4b) and (4c) demonstrate much faster decreasing of $\Delta B$ with increasing of $\sqrt{s}$ than that of the functions (4a) and (4d). At present the proton-proton experimental data at highest available energy 8 TeV do not contradict with fast (square of logarithm of energy) increasing of slope at high energies in the general case. Such behavior could agree with the asymptotic growth of total cross-section. Furthermore, in contrast with the previous analysis [9], here the quadratic logarithmic function (4d) leads to much smaller difference $\Delta B$ for $\overline{p}p$ and $pp$ scattering in high energy domain for both low (Figure 6(a)) and intermediate (Figure 6(b)) values of $|t|$. The only Regge-inspired function (4a) predicts the decreasing of $\Delta B$ with energy growth at intermediate $|t|$ (Figure 6(b)) for any values of $\sqrt{s}$. The parameterizations

Table 7: Predictions for slopes in $pp$ elastic scattering at high energies for intermediate $|t|$ domain.

| Fitting function | Facility energies $\sqrt{s}$, TeV | | | | | | |
|---|---|---|---|---|---|---|---|
| | RHIC | LHC | | | FCC/VLHC | | |
| | 0.5 | 14 | 28 | 42* | 100 | 200 | 500 |
| | $B$-parameter | | | | | | |
| (4a) | 12.8 ± 0.2 | 15.6 ± 0.3 | 16.2 ± 0.3 | 16.6 ± 0.4 | 17.3 ± 0.4 | 17.9 ± 0.4 | 18.7 ± 0.4 |
| (4b) | 12.4 ± 0.3 | 14.6 ± 0.4 | 15.1 ± 0.5 | 15.3 ± 0.5 | 15.9 ± 0.5 | 16.3 ± 0.6 | 16.9 ± 0.6 |
| (4c) | 13 ± 2 | 15 ± 3 | 16 ± 4 | 16 ± 4 | 17 ± 4 | 17 ± 4 | 18 ± 5 |
| (4d) | 14.5 ± 1.1 | 24 ± 2 | 27 ± 2 | 28 ± 3 | 32 ± 3 | 35 ± 3 | 40 ± 4 |
| | $b$-parameter | | | | | | |
| (4a) | 14.6 ± 0.6 | 18.8 ± 0.9 | 19.7 ± 1.0 | 20.2 ± 1.0 | 21.3 ± 1.1 | 22.2 ± 1.1 | 23.3 ± 1.2 |
| (4b) | 13 ± 4 | 16 ± 5 | 16 ± 5 | 17 ± 5 | 17 ± 6 | 18 ± 6 | 18 ± 6 |
| (4c) | 13.7 ± 1.9 | 17 ± 3 | 18 ± 3 | 18 ± 3 | 19 ± 3 | 20 ± 3 | 21 ± 4 |
| (4d) | 12 ± 5 | 9 ± 9 | 8 ± 10 | 7 ± 11 | 6 ± 12 | 4 ± 13 | 2 ± 14 |

*The ultimate energy upgrade of LHC project [4].

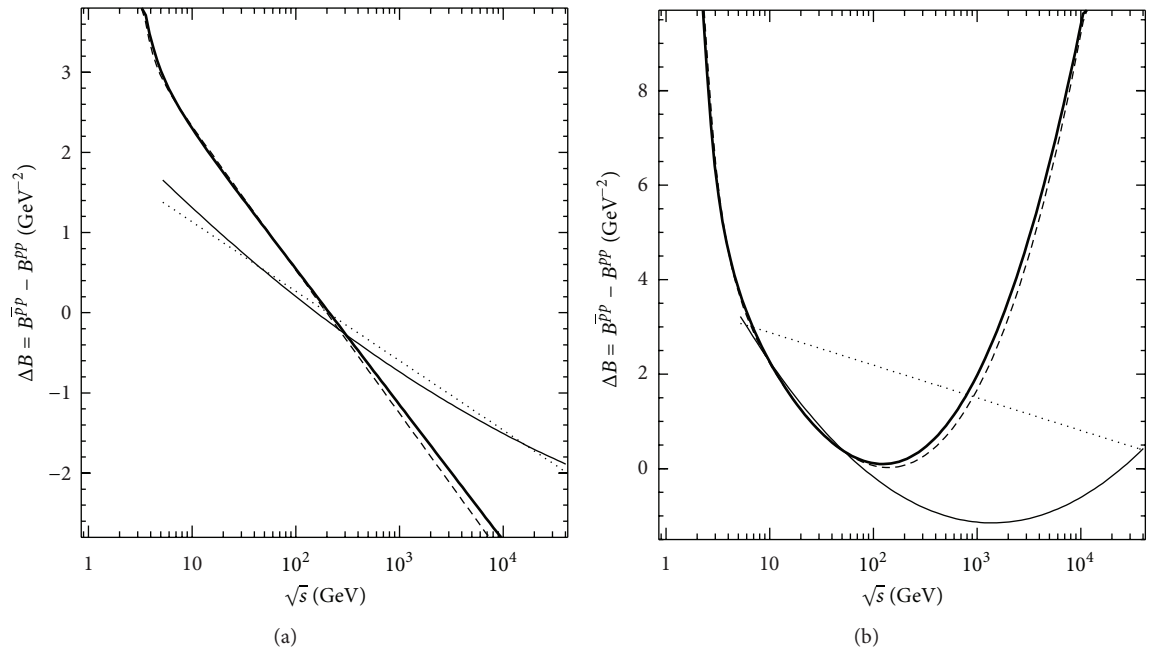


Figure 6: The energy dependence of the difference of elastic slopes for proton-antiproton and proton-proton scattering in low $|t|$ domain (a) and in intermediate $|t|$ range for linear exponential fit of differential cross-section (b). The correspondence of curves to the fit functions is the same as that in Figure 1.

(4b)–(4d) predict the decreasing of difference of slopes at low and intermediate energies and fast increasing of $\Delta B$ at high energies for intermediate $|t|$ domain (Figure 6(b)). As expected the slowest changing of $\Delta B$ is predicted by Regge-inspired function (4a) at asymptotic energies. All fitting functions with experimentally inspired parameters do not predict the constant zero values of $\Delta B$ at high energies. But it should be emphasized that only separate fits were made for experimental data for $pp$ and $\overline{p}p$ elastic reactions above. These results indicate on the importance of investigations at ultra-high energies both $pp$ and $\overline{p}p$ elastic scattering for study of many fundamental questions and predictions related to the general asymptotic properties of hadronic physics.

Also we have analyzed general data samples for $pp$ and $\overline{p}p$ elastic scattering. Slope parameters ($B$ and $b$) show a different energy dependence at $\sqrt{s} < 5$ GeV in proton-proton and antiproton-proton elastic reactions in any $|t|$ domains under study. Thus slopes for nucleon-nucleon data are investigated only for $\sqrt{s} \geq 5$ GeV below. We have included in fitted samples only $pp$ and $\overline{p}p$ points which were included in corresponding final data samples at separate study $pp$ and $\overline{p}p$ elastic reactions above. We did not exclude any points from $NN$ data sample; we change only the low energy boundary for fitted domain. Figure 7 shows the experimental data for slope in nucleon-nucleon elastic scattering against collision energy at low $|t|$. As seen from Figure 7 there is

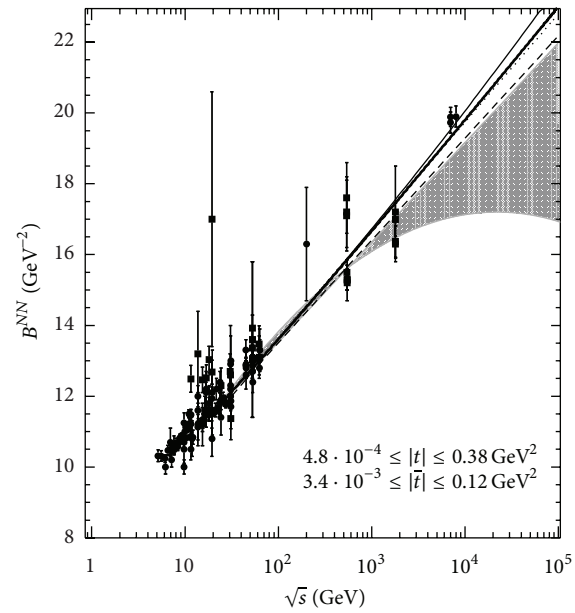


FIGURE 7: Energy dependence of the elastic slope parameter for nucleon-nucleon scattering for low $|t|$ domain. Experimental points from fitted samples are indicated as • for $pp$ and as ■ for $\overline{p}p$. Fits are shown for $\sqrt{s_{\min}} = 20$ GeV. The dot curve is the fit of experimental slope by the function (4a), thick solid—by (4b), dashed—by (4c), and thin solid—by (4d). The shaded band corresponds to the spread of fitting functions for previous analysis [9].

no experimental data for $\overline{p}p$ between $\sqrt{s} = 5$ GeV and $\sqrt{s} = 10$ GeV. This energy domain will be available for further FAIR facility. We have fitted the general nucleon-nucleon data sample at the range of low energy boundary $s_{\min} = 25, 100, 225$ and $400\,\text{GeV}^2$. The fitting parameter values are indicated in Table 8 on the first line for low boundary of the fitted energy domain $s_{\min} = 25\,\text{GeV}^2$ and on the second line for $s_{\min} = 400\,\text{GeV}^2$. The fit quality improves for most parameterizations under consideration at increasing of $s_{\min}$. One need to emphasize the fit quality is some poorer ($\chi^2$/n.d.f. $\simeq$ 2.3–2.9) at $\sqrt{s} \ge 10$ GeV than that for $\sqrt{s} \ge 5$ GeV for functions (4a) and (4c). For these cases of the fitted energy domain the value of the $a_1$ parameter obtained with the function (4a) agrees qualitatively with the Regge model prediction, but the value of the $a_1$ obtained at $s_{\min} = 400\,\text{GeV}^2$ is somewhat larger than the prediction for $\alpha'_{\mathscr{P}}$ from Pomeron-inspired model for TeV-energy domain [18]. Also results from fit by function (4d) with acceptable quality at $s_{\min} = 400\,\text{GeV}^2$ allow the estimation $2\alpha'_{\mathscr{P}}(s)|_{\sqrt{s}=8\,\text{TeV}} = 0.74 \pm 0.12$ which is some larger than the corresponding prediction from [18]. Furthermore the estimations for $2\alpha'_{\mathscr{P}}(s)|_{\sqrt{s}=8\,\text{TeV}}$ do not depend on $s_{\min}$ within error bars. Fitting functions (4a)–(4d) are shown at Figure 7 for $s_{\min} = 400\,\text{GeV}^2$. All functions (4a)–(4d) are close to each other at energies up to $\sqrt{s} \sim 1$ TeV at least and show quasi-linear behavior for parameter values obtained by fits with $s_{\min} = 25\,\text{GeV}^2$ and $s_{\min} = 400\,\text{GeV}^2$. As seen from comparison between the present fits and the spread of previous fit functions (shaded band) there is a dramatic change of behavior of the fitting function (4d) in comparison with previous analysis [9] due to experimental points at the LHC energies. At present the fitting function (4d) predicts increasing of the nuclear slope in high energy domain as well as all other fitting functions under study. Such behavior is opposite to the result of fit by function (4d) of experimental data sample at $\sqrt{s} \le 1.8$ TeV [9]. We have analyzed the nucleon-nucleon data for slope parameters $B$ and $b$ at intermediate $|t|$ values for linear and quadratic exponential parametrization of $d\sigma/dt$, respectively. Experimental $pp$ and $\overline{p}p$ data for $B$ differ significantly up to $\sqrt{s} \simeq 10$ GeV; at least that results in unacceptable fit qualities for all functions under study ($\chi^2$/n.d.f. $\simeq$ 28.9 for best fit by quadratic logarithmic function). Additional analysis demonstrates the improving of fit quality for (4b)–(4d) with increasing of low energy boundary from $s_{\min} = 25\,\text{GeV}^2$ up to $s_{\min} = 400\,\text{GeV}^2$. The values of fit parameters for the last case are shown in Table 9. The Regge-inspired function (4a) contradicts with experimental data. We would like to emphasize that the best fit quality for (4a) is obtained at $s_{\min} = 100\,\text{GeV}^2$ ($\chi^2$/n.d.f. $\simeq$ 9.45) but it is statistically unacceptable too. Functions (4b)–(4d) agree with experimental dependence $B(\sqrt{s})$ reasonably and have very close fit qualities. One can see from Table 9 that the statistically acceptable fits have been obtained for $b$-parameter at $s_{\min} = 400\,\text{GeV}^2$ only. Experimental data and fit functions are presented at Figure 8. Functions (4b)–(4d) show close fit qualities. Best fit is (4d) but "expanded" parameterizations agree with data too. One needs to emphasize that the significant errors and absence of experimental points at $\sqrt{s} \simeq 0.1$–$2$ TeV do not allow one to get the more clear conclusion. The RHIC as well as LHC data for nucleon-nucleon differential cross-section at intermediate $|t|$ will be helpful for distinguishing of various fit functions. One can conclude that the slope parameters for $pp$ and $\overline{p}p$ elastic scattering show universal behavior at $\sqrt{s} \ge 20$ GeV and "expanded" functions represent the energy dependencies for both low and intermediate $|t|$ ranges for this energy domain. Thus quantitative analysis of slopes at different $|t|$ allows us to get the following estimation of low energy boundary: $\sqrt{s} \simeq 20$ GeV for universality of elastic nucleon-nucleon scattering. This estimation agrees with results for differential cross-sections of $pp$ and $\overline{p}p$ elastic reactions based on the crossing-symmetry and derivative relations [2, 3].

## 3. Conclusions

The main results of this paper are the following. Energy dependence for several slope parameters is analyzed quantitatively for elastic nucleon-nucleon scattering in various $|t|$ domains. Most of all available experimental data samples for slope parameters in elastic nucleon collisions are approximated by different analytic functions.

The suggested new parameterizations allow us to describe experimental nuclear slope at all available energies in low $|t|$ domain for $pp$ quite reasonably. The new approximations agree with experimental $\overline{p}p$ data at qualitative level but these fits are still statistically unacceptable because of the very sharp behavior of $B$ near the low energy limit. The best fit qualities are obtained for suggested "expanded" functions

Table 8: Fitting parameters for slope energy dependence in low $|t|$ domain for $NN$ elastic scattering.

| Function | Parameter | | | | |
|---|---|---|---|---|---|
| | $B_0$, GeV$^{-2}$ | $a_1$, GeV$^{-2}$ | $a_2$, GeV$^{-2}$ | $a_3$ | $\chi^2$/n.d.f. |
| (4a) | $8.10 \pm 0.05$ | $0.301 \pm 0.004$ | — | — | 332/127 |
| | $7.55 \pm 0.05$ | $0.331 \pm 0.005$ | — | — | 103/63 |
| (4b) | $9.4 \pm 0.2$ | $6.1 \pm 1.1$ | $-12 \pm 2$ | $-3.5 \pm 1.5$ | 281/125 |
| | $8.1 \pm 0.7$ | $2.532 \pm 0.006$ | $-4.6 \pm 0.2$ | $0.988 \pm 0.015$ | 103/61 |
| (4c) | $8.15 \pm 0.09$ | $0.208 \pm 0.010$ | $0.50 \pm 0.09$ | $0.118 \pm 0.005$ | 281/125 |
| | $7.8 \pm 0.2$ | $0.323 \pm 0.009$ | $-7.0 \pm 1.7$ | $-0.65 \pm 0.15$ | 102/61 |
| (4d) | $8.81 \pm 0.12$ | $0.204 \pm 0.015$ | $0.011 \pm 0.002$ | — | 286/126 |
| | $8.0 \pm 0.3$ | $0.28 \pm 0.04$ | $0.005 \pm 0.003$ | — | 101/62 |

Table 9: Fitting parameters for energy dependence of slope parameters at intermediate $|t|$ for $NN$ elastic scattering.

| Function | Parameter | | | | |
|---|---|---|---|---|---|
| | $B_0$, GeV$^{-2}$ | $a_1$, GeV$^{-2}$ | $a_2$, GeV$^{-2}$ | $a_3$ | $\chi^2$/n.d.f. |
| | | | $B$-parameter | | |
| (4a) | $5.17 \pm 0.11$ | $0.369 \pm 0.006$ | — | — | 353/36 |
| (4b) | $10.7 \pm 0.2$ | $-0.019 \pm 0.011$ | $(1.04 \pm 0.17) \times 10^{-4}$ | $4.08 \pm 0.08$ | 107/34 |
| (4c) | $10.5 \pm 0.2$ | $-0.165 \pm 0.019$ | $0.66 \pm 0.06$ | $0.187 \pm 0.004$ | 106/34 |
| (4d) | $14.9 \pm 0.6$ | $-0.61 \pm 0.06$ | $0.089 \pm 0.006$ | — | 118/35 |
| | | | $b$-parameter | | |
| (4a) | $6.97 \pm 0.13$ | $0.318 \pm 0.012$ | — | — | 221/40 |
| | $6.8 \pm 0.5$ | $0.31 \pm 0.03$ | — | — | 15.3/7 |
| (4b) | $7.5 \pm 0.2$ | $0.282 \pm 0.017$ | $-595 \pm 662$ | $-6 \pm 3$ | 206/38 |
| | $-23 \pm 8$ | $0.98 \pm 0.19$ | $144 \pm 40$ | $-1 \pm 2$ | 2.43/5 |
| (4c) | $7.5 \pm 0.2$ | $0.281 \pm 0.016$ | $-152 \pm 287$ | $-1.7 \pm 0.6$ | 205/38 |
| | $9.0 \pm 28.5$ | $-1.7 \pm 1.4$ | $13 \pm 31$ | $0.10 \pm 0.08$ | 2.40/5 |
| (4d) | $6.5 \pm 0.3$ | $0.40 \pm 0.04$ | $-0.010 \pm 0.005$ | — | 217/39 |
| | $26 \pm 5$ | $-1.6 \pm 0.5$ | $0.17 \pm 0.05$ | — | 2.40/6 |

both for $pp$ and $\overline{p}p$ data. The obtained values of asymptotic shrinkage parameter $\alpha'_{\mathcal{P}}$ for $pp$ elastic scattering are larger than $\alpha'_{\mathcal{P}}$ values for elastic $\overline{p}p$ reactions for the Pomeron-inspired fitting function. Various approximations differ from each other both in the low energy and very high energy domains. Predictions for slope parameter are obtained for elastic proton-proton and proton-antiproton scattering in energy domains of some facilities at low momentum transfer. Our predictions based on the all available experimental data do not contradict the phenomenological model estimations qualitatively. The situation is more unclear at intermediate $|t|$ values than that at low $|t|$ domain. Only the qualitative agreement is observed between approximations and experimental points both for $pp$ and $\overline{p}p$ collisions for linear exponential parametrization of $d\sigma/dt$ because of poorer quality of data. The "expanded" functions describe $pp$ data for $B$-parameter for any differential cross-section parametrization reasonably. Best fit quality is obtained for quadratic function of logarithm for the $pp$ data from any exponential parametrization of $d\sigma/dt$. One needs to emphasize that this fit function allows us to describe $\overline{p}p$ data at all available energies and shows a statistically acceptable fit quality for data sample obtained from quadratic exponential parametrization of $d\sigma/dt$. Slope parameter $b$ calculated at $|t| = 0.2\,\text{GeV}^2$ shows more smooth energy dependence. We have obtained acceptable fit qualities for "expanded" functions both for $pp$ and $\overline{p}p$ data at all initial energies. The obtained values of shrinkage parameter $a_1$ for $pp$ elastic scattering are close to the early results for intermediate $|t|$ domain. As well as for low $|t|$ domain predictions for slope parameters $B$ and $b$ are obtained for elastic proton-proton and proton-antiproton scattering in energy domains of some facilities. It seems the phenomenological model with hadronic amplitude corresponding to the exchange of three Pomerons describes the nuclear slope somewhat closer to the experimental fit inspired values at the LHC energy both at low and intermediate $|t|$ than other models.

The energy dependence of difference of slopes ($\Delta B$) for proton-antiproton and proton-proton elastic scattering was obtained for fitting functions under study. The $\Delta B$ parameter shows the opposite behaviors at high energies for low and intermediate $|t|$ domains (decreasing/increasing, resp.) for all fitting functions with the exception of Regge-inspired one. The last function predicts the slow decreasing of $\Delta B$ with energy growth. It should be emphasized that all underlying empirical fitting functions with experimentally inspired parameter values do not predict the zero difference of slopes for proton-antiproton and proton-proton elastic scattering both at low and intermediate $|t|$ for high energy domain.

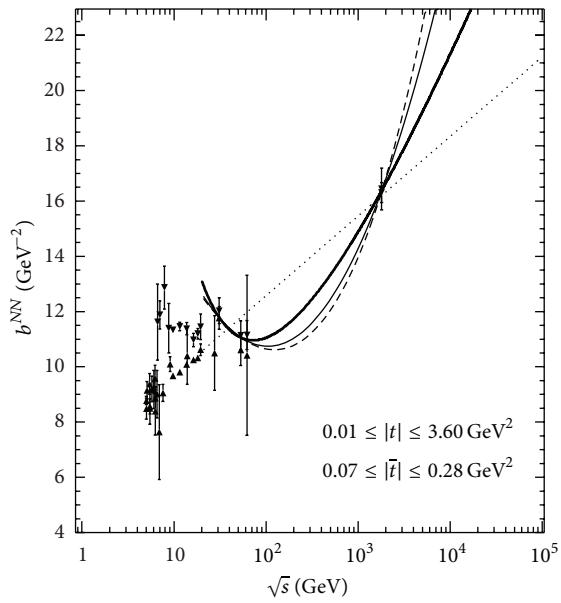


Figure 8: Energy dependence of the elastic slope parameter $b$ at $|t| = 0.2\,\text{GeV}^2$ for nucleon-nucleon scattering for intermediate $|t|$ domain. Experimental fitted points are indicated as ▲ for $pp$ and as ▼ for $\overline{p}p$. Fits are shown for $\sqrt{s_{\min}} = 20$ GeV. The correspondence of curves to the fit functions is the same as that in Figure 1.

We have analyzed general nucleon-nucleon data samples for slopes at $\sqrt{s} \ge 5$ GeV. The "expanded" functions show the statistically acceptable fit qualities at $\sqrt{s} \ge 20$ GeV for low $|t|$ domain. Slop analysis allows us to find the following value $0.331 \pm 0.005$ for $\alpha'_{\mathscr{P}}$ parameter. The estimation of asymptotic shrinkage parameter $\alpha'_{\mathscr{P}}$ obtained with quadratic function of logarithm for $NN$ data at $\sqrt{s} = 8$ TeV is noticeably larger than the expectation from the Pomeron theory. But the growth of $\alpha'_{\mathscr{P}}$ with increasing of $\sqrt{s}$ is observed from the comparison of the fit results from present analysis and our earlier analysis for $\sqrt{s} \le 1.8$ TeV. Such behavior of $\alpha'_{\mathscr{P}}$ agrees with Pomeron-inspired model. Functions (4c) and (4d) represents experimental $NN$ data for $B$ and $b$ slope parameters, respectively, at intermediate $|t|$ with best quality. But the function (4b) shows close qualities and agrees with data reasonably. Therefore the suggested "expanded" functions can be used as reliable fits for wide range of momentum transfer at all energies. The universal behavior was found for available experimental $pp$ and $\overline{p}p$ slopes at $\sqrt{s} \ge 20$ GeV both for low and intermediate $|t|$ that is in agreement with the hypothesis of a universal shrinkage of the hadronic diffraction cone at high energies.

## Conflict of Interests

The author declares that there is no conflict of interests regarding the publication of this paper.

## References


[1] R. F. Ávila, S. D. Campos, M. J. Menon, and J. Montanha, "Phenomenological analysis connecting proton-proton and antiproton-proton elastic scattering," *European Physical Journal C*, vol. 47, no. 1, pp. 171–186, 2006.

[2] S. B. Nurushev and V. A. Okorokov, " Elastic proton-proton and proton-antiproton scattering: analysis of complete set of helicity amplitudes," http://arxiv.org/abs/arXiv:0711.2231.

[3] S. B. Nurushev and V. A. Okorokov, in *Proceedings of the 12th Advanced Research Workshop on High Energy Spin Physics*, A. V. Efremov and S. V. Goloskokov, Eds., p. 117, Dubna, Russia, 2008.

[4] A. N. Skrinsky, in *Proceedings of the 33rd International Conference of High Energy Physics*, A. Sissakian, G. Kozlov, and E. Kolganova, Eds., vol. 1, p. 175, World Scientific, 2007.

[5] V. A. Okorokov, "Diffraction slopes for elastic proton-proton and proton-antiproton scattering," http://arxiv.org/abs/0811.0895.

[6] V. A. Okorokov, "Slope analysis for elastic proton-proton and proton-antiproton scattering," http://arxiv.org/abs/0811.3849.

[7] M. M. Block and R. N. Cahn, "High-energy $p\overline{p}$ and $pp$ forward elastic scattering and total cross sections," *Reviews of Modern Physics*, vol. 57, p. 563, 1985.

[8] J. P. Burq, M. Chemarin, M. Chevallier et al., "Soft $\pi^-$p and pp elastic scattering in the energy range 30 to 345 GeV," *Nuclear Physics B*, vol. 217, no. 2, pp. 285–335, 1983.

[9] V. A. Okorokov, "Slope analysis for elastic nucleon-nucleon scattering," http://arxiv.org/abs/0907.0951.

[10] V. M. Abazov and DØ Collaboration, "Measurement of the differential cross section $d\sigma/dt$ in elastic $p\overline{p}$ scattering at $\sqrt{s} = 1.96$ TeV," *Physical Review D*, vol. 86, Article ID 012009, 2012.

[11] G. Antchev, P. Aspell, I. Atanassov et al., "Proton-proton elastic scattering at the LHC energy of $\sqrt{s} = 7$ TeV," *Europhysics Letters*, vol. 95, no. 4, Article ID 41001, 2011.

[12] G. Antchev, P. Aspell, I. Atanassov et al., "Measurement of proton-proton elastic scattering and total cross-section at $\sqrt{s} = 7$ TeV," *Europhysics Letters*, vol. 101, no. 2, Article ID 21002, 2013.

[13] G. Antchev, P. Aspell, I. Atanassov et al., "Luminosity-independent measurement of the proton-proton total cross section at $\sqrt{s_{NN}} = 8$ TeV," *Physical Review Letters*, vol. 111, Article ID 021001, 2013.

[14] G. Aad, B. Lemmer, R. Pöttgen et al., "Measurement of the total cross section from elastic scattering in pp collisions at $\sqrt{s} = 7$ TeV with the ATLAS detector," *Nuclear Physics B*, vol. 889, pp. 486–548, 2014.

[15] T. Lasinski, R. L. Setti, B. Schwarzschild, and P. Ukleja, "Energy dependence of the elastic diffraction slopes," *Nuclear Physics B*, vol. 37, no. 1, pp. 1–58, 1972.

[16] M. M. Block, "Hadronic forward scattering: predictions for the Large Hadron Collider and cosmic rays," *Physics Reports*, vol. 436, pp. 71–215, 2006.

[17] F. Abe, M. Albrow, D. Amidei et al., "Measurement of small angle antiproton-proton elastic scattering at $\sqrt{s} = 546$ and 1800 GeV," *Physical Review D*, vol. 50, no. 9, pp. 5518–5534, 1994.

[18] V. A. Schegelsky and M. G. Ryskin, "Diffraction cone shrinkage speed up with the collision energy," *Physical Review D*, vol. 85, Article ID 094024, 2012.

[19] G. Giacomelli, "Total cross sections and elastic scattering at high energies," *Physics Reports*, vol. 23, no. 2, pp. 123–235, 1976.

[20] V.Kundrát, J.Kašpar, and M.Lokajícek, in *Proceedings of the 12th International Conference on Elastic and Diffractive Scattering Forward Physics and QCD*, J. Bartels, M. Diehl, and H. Jung, Eds., p. 273, DESY, 2007.

[21] M. M. Block, E. M. Gregores, F. Halzen, and G. Pancheri, "Photon-proton and photon-photon scattering from nucleon-nucleon forward amplitudes," *Physical Review D*, vol. 60, Article ID 054024, 1999.

[22] V. A. Petrov, E. Predazzi, and A. V. Prokhudin, "Coulomb interference in high-energy pp and anti-pp scattering," *The European Physical Journal C*, vol. 28, pp. 525–533, 2003.

[23] C. Bourrely, J. Soffer, and T. T. Wu, "Impact-picture phenomenology for $\pi^{\pm}p$, $K^{\pm}p$ and $pp$, $\overline{p}p$ elastic scattering at high energies," *The European Physical Journal C*, vol. 28, pp. 97–105, 2003.

[24] M. M. Islam, R. J. Luddy, and A. V. Prokhudin, "$pp$ elastic scattering at LHC in near forward direction," *Physics Letters B*, vol. 605, pp. 115–122, 2005.

[25] O. V. Selyugin and J.-R. Cudell, in *Proceedings of the 12th International Conference on Elastic and Diffractive Scattering Forward Physics and QCD*, J. Bartels, M. Diehl, and H. Jung, Eds., p. 279, Verlag DESY, 2007.

[26] S. D. Campos and V. A. Okorokov, "Analysis of $\overline{p}p$ and elastic scattering based on high energy bounds," *International Journal of Modern Physics A*, vol. 25, no. 29, pp. 5333–5348, 2010.

[27] N. A. Amos, C. Avila, W. F. Baker et al., "Antiproton-proton elastic scattering at $\sqrt{s} = 1.8$ TeV from $|t| = 0.034$ to 0.65 $(\text{GeV}/c)^2$," *Physics Letters B*, vol. 247, no. 1, pp. 127–130, 1990.